Theoretical and Computational Acoustics
D. Lee, Y-H Pao, M.H. Schultz, and Y-C Teng (Editors)

The Impact of Mesoscale Oceanic Structure on Global-Scale Acoustic Propagation

E.C. Shang and Y.Y. Wang
CIRES, University of Colorado/NOAA/Environmental Technology Lab.

Abstract

The variability of acoustic field associated with mesoscale oceanic structures affects as "noise" for global-scale monitoring. A better understanding of the acoustic variability caused by mesoscale oceanic structures would be helpful for data interpretation and the final estimation of the global trend. In this paper, the nonlinearity of modal travel time perturbation and the mode-coupling impact on travel time are discussed. It is found that higher mode at lower frequency wii be more robust under mesoscale disturbance.

(1). INTRODUCTION

The variability of acoustic field associated with mesoscale oceanic structures affects as "noise" for global-scale monitoring. Actually, the ability to measure temperature change in ocean due to climate change - (ATOC) [1] is largely limited by the presence of mesoscale variability.

The trouble is the fact that the acoustic variability caused by mesoscale eddies can not be averaged out even over a long path/period. The travel time perturbation is nonlinear, the mode-coupling impact is also nonlinear , which means that even the averaged ocean temperature perturbation is zero but the net travel time perturbation is not zero. Furthermore, some of the important acoustic features (e.g. arrival order, dispersion) can be changed drastically compared with the "range-averaged" medium [2].

In this paper, the nonlinearity of modal travel time perturbation and the impact of mode-coupling on travel time are discussed and some results of numerical simulation are presented.

The ocean model for numerical simulations consists of a canonical Munk profile [3] as the background and a Gaussian eddy as perturbation :

$$C_0(z) = 1500\{1 + 0.0057[e^{-\eta} - (1-\eta)]\},$$

$$\delta C(r, z) = DC \cdot \exp\left[-\left(\frac{r - r_e}{DR}\right)^2 - \left(\frac{z - z_e}{DZ}\right)^2\right],$$

where $\eta = 2(z - 1000)/1000.$

The Gaussian eddy parameters for different cases are listed in Table 1. Because the depth of eddy is a sensitive parameter, we consider two types :

(A). z_e = 1000 m (on axis eddy),
(B). z_e = 700 m (off axis eddy).

For the former case, a "double channel" exists for warm eddy, and for the later case there is no "double channel" (see Fig.1 and Fig.2). In order to get a clear dependency of the nonlinearity with eddy strength, parameter (DC) has been varied from 1.5 (m/s) to 15.0 (m/s) through 8 steps both for warm and cold eddy.

(2). NONLINEARITY AND TRAVEL TIME BIAS

The nonlinear constituent of acoustic travel time perturbation in ocean is significant for many cases of interest [4-7]. Linearized inversion which uses the exact travel time perturbation for data should yield biased results. A better understanding of nonlinearity of travel time perturbation is important for data interpreting and establishing a proper scheme of inversion of tomography.

The formulations for calculating the exact (nonlinear) travel time perturbation and the linearized travel time perturbation of adiabatic mode are given by eq.(1) and eq.(2) as follows :

$$dt_m = \int dr \left\{ \tilde{C}_m \int_0^{\infty} \tilde{\psi}_m^2 \frac{1}{\tilde{C}^2} dz - C_m \int_0^{\infty} \psi_m^2 \frac{1}{C^2} dz \right\}. \qquad (1)$$

$$dt_m^{(L)} = \int_0^{R} dr \left\{ \frac{\partial}{\partial \omega} \left(\frac{-\omega_0^2}{k_m} \cdot \int_0^{\infty} \psi_m^2 \left(\frac{\Delta c}{c^3} \right) dz \right) \right\}. \qquad (2)$$

where $\tilde{C}_m$ and $\tilde{\Psi}_m$ are the perturbed modal phase velocity and modal eigenfunction corresponding to the perturbed SSP given by

$$c(z,r) = c_0(z) + \Delta c(z,r)$$

and C_m, Ψ_m are the unperturbed modal phase velocity, eigenfunction corresponding to the "background" SSP $c_0(z)$ respectively. As we can see from Eq.(1), that the exact travel time has a nonlinear relationship with $\Delta c(z,r)$, because $\tilde{C}_m$ and $\tilde{\Psi}_m$ are also depend on $\Delta c(z,r)$.

The nonlinearity of modal travel time perturbation can be described by an indicator - N_e defined as follows

$$N_e = \frac{dt_m - dt_m^{(L)}}{dt_m^{(L)}} \qquad (3)$$

Three features of the nonlinearity can be expressed by this indicator :

1). the relative magnitude (percentage) of the nonlinear constituent,
2). the orintation of the nonlinear bias :
if $N_e > 0$, then "cold" bias,
if $N_e < 0$, then "warm" bias,
3). the (DC) dependency of the nonlinearity.

To illustrate the (DC) (eddy strength) dependency of the nonlinearity, let us write dt_m as a sum of the linear constituent and a non-linear constituent

$$dt_m = dt_m^{(L)} + dt_m^{(NL)} \tag{4}$$

Substituting Eq.(4) into Eq.(3), yields

$$Ne = \frac{dt_m^{(NL)}}{dt_m^{(L)}} \tag{5}$$

Let us assume a "power law" for the nonlinear constituent as follows

$$dt_m^{(NL)} \sim B_m (DC)^n \tag{6}$$

and for the linear constituent

$$dt_m^{(L)} \sim A_m (DC) \tag{7}$$

Then, we have

$$Ne \sim (B_m/A_m) (DC)^{n-1} \tag{8}$$

As examples, some of the numerical results of nonlinearity are listed on Table 2 and Table 3. The mode number dependency for cases of (A8-), (A8+) and (B8+) are illustrated on Fig.3. The frequency dependency for case (A8+) is illustrated on Fig.4. The eddy strength (DC) dependency for warm/cold and on-axis/off-exis cases are illustrated on Fig. 5-8. Where a "normalized" values defined as follows

$$Nn = Ne/Max(Ne) \tag{9}$$

$$(DC)n = (DC)/Max(DC) \tag{10}$$

are used. The "square" law (n=2) should be the *diagonal* in Fig.5-8. As we can see that the power of the nonlinear constituent is not as expected $n = 2$, but roughly

$$n \sim (1.5 - 3.0)$$

for cold eddy, and for warm eddy it some times even is not monotonic. At this point, we are not able to explain it.

(3). MODE-COUPLING IMPACT

For ocean acoustic thermometry [1], it is important to know how the acoustic wave samples the ocean and then a clear relationship between the travel time measurement and the ocean temperature information can be established. been known for an adiabatic mode regime, the linearized formula is

$$dt_m^{(AD)} = \int_o^R dr\left\{\int T_m^o(z)\delta c(z,r)dz\right\}. \tag{11}$$

Where $dt_m^{(AD)}$ is the adiabatic modal travel time perturbation referred to a known background ocean model and T_m^0 is the kernel function calculated with the background ocean model

$$T_m^o(z) = \frac{\partial}{\partial w}\left[\frac{-w_o^2}{k_m^o}\left|z_m^o(z)\right|^2 \cdot \frac{1}{c_o^3(z)}\right]. \tag{12}$$

Therefore, the range-averaged sound speed perturbation defined as

$$\overline{\delta C^{(G)}}(z) = \int_O^R \delta C^{(G)}(r,z)dr, \tag{13}$$

can be obtained from this vertical slice tomography by inversion, and the range-averaged temperature perturbation is given by a simple linear transformation.

On the otherhand, if mode coupling takes place along the propagation path, then the modal travel time perturbation has no simple relationship to the sound speed perturbation because of mode-mode scattering mixed up the modal features - modal amplitude; modal phase/travel time. Inversion of the temperature information from the non-adiabatic modal travel time remaines a challenge for ocean acoustic tomography. Recently, efforts along this direction have been made [8].

Consequently, to investigate the adiabaticity of acoustic propagation becomes a very important issue for the acoustic thermometry system design and data interpretation.

The term of "adiabaticity" is a word we use to describe how the acoustic propagation is close to the propagation of adiabatic mode. In literature, adiabaticity has been discussed by establishing a criterion [9] :

$$M >> D_{mn} \tag{14}$$

where two characteristic scales are involved

M - scale of the ocean variability,
D_{mn} - scale of modal interference distance, defined as

$$D_{mn} = 2\pi / (k_m - k_n) \tag{15}$$

We found that D_{mn} is a crucial factor determining adiabaticity. Critical mode coupling occurs when D_{mn} goes to infinite, which corresponding to the situation of modal *degeneration* - ($k_m \rightarrow k_n$) it often takes place in "double channel" .

The mode-coupling matrix for a weak warm eddy (case A4+) and a strong warm eddy (case A8+) have been calculated by using the MOSPEF method [10]. The IFD-WAPE code [11] is used for the propagating field and the KRAKEN normal mode code [12] is used for generating the initial single mode as input and the decomposition of the final field as output. Results are listed on Table 4 and Table 5, and the travel time impacts are listed on Table 6 and Table 7 respectively. The corresponding D_{mn} variations are illustrated on Fig.9 and Fig.10.

The "critical" coupling point for lower modes (m= 1 - 6) can be clearly found in Fig.10, but not in Fig.9. This is because a (DC)=5 m/s warm eddy is not strong enough to split the SOFAR channel into a "double channel" to produce modal *degeneration* at this 50 Hz frequency. The evidence of the "double channel" effect can also be found for the case of (B8+) where we have the same strong warm eddy as in case of (A8+) ((DC) =12.5 m/s) but because the center raised to Ze = 700 m, then the "double channel" disappeared (see Fig.11a) and the critical points of D_{mn} disappeared (see Fig.11b). Consequently, the mode-coupling impact on travel time disappeared (see Table 8). So, our conclusion is : *No double channel , no strong mode coupling !*

SUMMARY

(1). The nonlinearity of modal travel time perturbation has a complex dependency on eddy parameters and mode numbers, specialy it is sensitive to the depth of eddy. The dependence on eddy strength is not as expected a square law.
(2). In our simulation cases, most (not always) of the biases are cold.
(3). The applicability of linearized travel time perturbation formula is very limited. For a weaker mesoscale eddy (DC= 5 m/sec) the error is about 10 ms, and for a stronger mesoscale eddy (DC=12 m/sec) the error is about 100 ms .
(4). Strong mode-coupling takes place where a strong enough "double channel" exists (e.g. a strong on-axis warm eddy). In contrast with adiabatic mode, the non-adiabatic mode suffers :
    . repopulation
    . rough dispersion - changed arrival order
    . initial condition (source depth) dependent
(5). Higher modes are relatively robust to the mesoscale perturbation, and it could be more robust if the frequency goes down (say 20 Hz). It will be good for ATOC.

Acknowledgement: This work was supported by ARPA, ONR and NOAA.

References

[1]. W.H. Munk, "Global acoustics," J. Acoust. Soc. Am., 95, No.5, Pt.2, 2849, 1994.
[2]. E.C. Shang, Y.Y. Wang and T.M. Georges,"Dispersion and repopulation of Heard-Ascension modes," J. Acoust. Soc. Am., 96, pp.2371-2379, 1994.
[3]. W.H. Munk, "Sound channel in an exponential stratified ocean with application of SOFAR ," J. Acoust. Soc. Am.,55, pp.220-226, 1974.
[4]. J. Mercer and J. Booker, "Long-range propagation of sound through oceanic mesoscale structure," J. G. R. 88, pp.689-699, 1983.
[5]. J. Spiesberger and P. Worcester, "Perturbation in travel time and ray geometry due to meso-scale disturbances," J. Acoust. Soc. Am., 74, pp. 219-225, 1983.
[6]. W. Munk and C. Wunsch,"Biases and caustics in long-range acoustic tomography," Deep Sea Res., 32, pp.1316-1346, 1985.
[7]. E.C. Shang and Y.Y. Wang, "The nonlinearity of modal travel time perturbation," *Computa-tioan Acoustics,* Ed. R. Lau, D. Lee and A. Robinson, pp.385-397, 1993. Elsevier Science Publishers B.V. (North-Holland).
[8]. C.S. Chiu et al, "Inverse techniques for coastal acoustic tomography," Proceedings of the International Conference on Theoretical and Computatioal Acoustics, Mystic, Connecticut 1993. Ed. D. Lee.
[9]. L.Brekhovskikh and Yu. Lysanov, "Fundamentals of Ocean Acoustics," Springer, 1982.
[10]. E.C. Shang and Y.Y. Wang, "Acoustic travel time computation based on PE solution," J. Comput. Acoust. ,Vol.1. pp.91-100, 1993.
[11]. D. Lee and G. Botseas, "An implicit finite-difference (IFD) computer model for solving the parabolic equation," NUSC Tech. Rep. 6659, 1982.
[12]. M. Poter, "The KRAKEN normal mode program," SACLANT Undersea Res. Center 1988.

Table 1. The eddy parameters and case numbers.

DR = 100 km
DZ = 500 m

(A). On axis eddy z = 1000 m		(B). Off axis eddy z = 700 m	
Case No.	(DC) m/s	Case No.	(DC) m/s
A1+	+ 1.5	B1+	+ 1.5
A1-	- 1.5	B1-	- 1.5
A2+	+ 2.0	B2+	+ 2.0
A2-	- 2.0	B2-	- 2.0
A3+	+ 3.125	B3+	+ 3.125
A3-	- 3.125	B3-	- 3.125
A4+	+ 5.0	B4+	+ 5.0
A4-	- 5.0	B4-	- 5.0
A5+	+ 6.25	B5+	+ 6.25
A5-	- 6.25	B5-	- 6.25
A6+	+ 7.5	B6+	+ 7.5
A6-	- 7.5	B6-	- 7.5
A7+	+ 10.0	B7+	+ 10.0
A7-	- 10.0	B7-	- 10.0
A8+	+ 12.5	B8+	+ 12.5
A8-	- 12.5	B8-	- 12.5
A9+	+ 15.0	B9+	+ 15.0
A9-	- 15.0	B9-	- 15.0

Table 2. The nonlinearity of modal travel time perturbations for on-axis eddy at 50 Hz.

	case A3+ (DC= +3.125 m/s)			case A3- (DC=-3.125 m/s)		
m	δt_m (ms)	$\delta t_m^{(L)}$ (ms)	Ne (%)	δt_m (ms)	$\delta t_m^{(L)}$ (ms)	Ne (%)
1	-244.49	-245.19	0.29	245.97	245.21	0.31
2	-237.91	-241.59	1.52	243.29	241.63	0.69
3	-227.24	-234.28	3.00	237.96	234.29	1.57
4	-215.15	-224.06	3.98	229.91	224.09	2.60
5	-202.77	-212.09	4.39	219.71	212.10	3.59
6	-190.69	-199.46	4.40	207.91	199.44	4.25
7	-179.22	-186.89	4.10	195.36	186.73	4.62
8	-168.59	-174.91	3.62	182.75	174.87	4.53
9	-158.60	-163.86	3.21	171.14	163.97	4.37
10	-149.97	-154.01	2.62	159.80	153.90	3.83
	case A5+ (DC=+6.25 m/s)			case A5- (DC=-6.25 m/s)		
1	-464.62	-490.38	5.25	493.14	490.41	0.56
2	-462.72	-483.20	4.24	488.69	483.24	1.13
3	-435.08	-468.57	7.15	479.95	468.58	2.41
4	-412.50	-448.14	7.95	466.89	448.18	4.17
5	-389.34	-424.18	8.22	449.81	424.20	6.04
6	-367.48	-398.91	7.88	429.18	398.87	7.60
7	-346.83	-373.70	7.19	406.08	373.54	8.71
8	-327.77	-349.78	6.29	381.46	349.70	9.08
9	-310.05	-327.77	5.40	356.83	327.86	8.83
10	-294.36	-307.93	4.41	332.73	307.86	8.08
	case A8+ (DC=+12.5 m/s)			case A8- (DC=-12.5 m/s)		
1	-717.47	-980.79	26.85	990.03	980.82	0.94
2	-725.93	-966.40	24.88	983.34	966.45	1.75
3	-744.26	-937.15	20.58	970.34	937.16	3.54
4	-811.56	-896.30	9.45	950.96	896.35	6.09
5	-713.93	-848.36	15.85	925.40	848.39	9.08
6	-742.89	-797.81	6.88	893.75	797.77	12.03
7	-677.56	-747.32	9.33	856.71	747.16	14.66
8	-647.80	-699.53	7.36	814.88	699.45	16.50
9	-613.88	-655.60	6.36	769.65	655.69	17.30
10	-582.36	-615.88	5.44	721.67	615.77	17.20

Table 3. The nonlinearity of modal travel time perturbations for off-axis at 50 Hz.

m	δt_m (ms)	$\delta t_m^{(L)}$ (ms)	Ne (%)	δt_m (ms)	$\delta t_m^{(L)}$ (ms)	Ne (%)
	Case B3+ (DC=+3.125 m/s)			Case B3- (DC=-3.125 m/s)		
1	-147.31	-170.94	13.82	189.01	170.96	10.56
2	-147.08	-167.65	12.27	184.90	167.68	10.27
3	-146.37	-162.65	10.01	177.93	162.65	9.39
4	-145.13	-157.02	7.58	169.58	157.06	7.98
5	-143.17	-151.41	5.44	160.95	151.42	6.29
6	-140.85	-146.19	3.65	152.90	146.17	4.61
7	-138.05	-141.28	2.28	145.83	141.15	3.31
8	-135.10	-136.77	1.22	139.70	136.69	2.21
9	-131.64	-132.56	0.69	134.71	132.66	1.54
10	-128.56	-128.68	0.09	129.86	128.61	0.98
	Case B5+ (DC=6.25 m/s)			Case B5- (DC= -6.25 m/s)		
1	-250.76	-341.89	26.65	400.72	341.90	17.20
2	-252.89	-335.31	24.58	393.68	335.35	17.39
3	-256.50	-325.29	21.24	380.57	325.30	16.99
4	-260.66	-314.07	17.00	362.91	314.10	15.54
5	-264.45	-302.84	12.68	343.04	302.86	13.27
6	-266.69	-292.37	8.69	322.84	292.34	10.43
7	-267.38	-282.50	5.35	304.40	282.38	7.80
8	-265.80	-273.51	2.82	288.33	273.41	5.46
9	-262.18	-265.16	1.12	274.96	265.26	3.66
10	-257.90	-257.34	-0.22	263.30	257.28	2.34
	Case B8+ (DC=12.5 m/s)			Case B8- (DC= -12.5 m/s)		
1	-387.69	-683.78	43.30	854.03	683.80	24.89
2	-391.72	-670.64	41.59	844.29	670.68	25.89
3	-399.06	-650.57	38.66	825.33	650.58	26.86
4	-409.03	-628.14	34.88	797.60	628.17	26.97
5	-420.95	-605.69	30.50	762.17	605.59	25.83
6	-434.29	-584.74	25.27	720.79	584.70	23.27
7	-448.43	-564.96	20.63	676.35	564.81	19.75
8	-463.18	-546.95	15.32	631.91	546.87	15.55
9	-477.49	-530.38	9.97	591.22	530.46	11.45
10	-490.94	-514.65	4.61	555.55	514.57	7.96

Table 4. Mode-coupling matrix for case A4+ (DC=+5.0 m/s) at 50 Hz.

Input		Output A									
A	M\N	1	2	3	4	5	6	7	8	9	10
1.0	1	.95	.25	.002	.0	.0	.0	.0	.0	.0	.0
1.0	2	.25	.95	.006	.0	.0	.0	.0	.0	.0	.0
1.0	3	.002	.006	.98	.002	.0	.0	.0	.0	.0	.0
1.0	4	.0	.0	.002	.98	.001	.0	.0	.0	.0	.0
1.0	5	.0	.0	.0	.0	.98	.0	.0	.0	.0	.0
1.0	6	.0	.0	.0	.0	.0	.98	.0	.0	.0	.0
1.0	7	.0	.0	.0	.0	.0	.0	.98	.0	.0	.0
1.0	8	.0	.0	.0	.0	.0	.0	.0	.98	.0	.0
1.0	9	.0	.0	.0	.0	.0	.0	.0	.0	.98	.0
1.0	10	.0	.0	.0	.0	.0	.0	.0	.0	.0	.98

Table 5. Mode-coupling matrix for case A8+ (DC=+12.5 m/s) at 50 Hz.

Input		Output A									
A	M\N	1	2	3	4	5	6	7	8	9	10
1.0	1	.58	.64	.43	.17	.028	.016	.0	.0	.0	.0
1.0	2	.64	.22	.64	.30	.052	.028	.010	.0	.0	.0
1.0	3	.43	.64	.42	.44	.092	.045	.016	.0	.0	.0
1.0	4	.17	.30	.44	.72	.35	.12	.043	.002	.0	.0
1.0	5	.028	.052	.092	.35	.67	.58	.19	.009	.0	.0
1.0	6	.016	.028	.045	.12	.58	.59	.50	.029	.0	.0
1.0	7	.0	.009	.015	.043	.19	.50	.82	.074	.005	.0
1.0	8	.0	.0	.0	.002	.009	.029	.074	.97	.074	.0
1.0	9	.0	.0	.0	.0	.0	.0	.006	.074	.98	.012
1.0	10	.0	.0	.0	.0	.0	.0	.0	.0	.011	.98

Table 6. Modal travel time perturbation for case A4+ (DC=+5.0 m/s) at 50 Hz.

M	Adiabatic δt_m^{Ad}(ms)	MOSPEF δt_m^{PE}(ms)	Coupling impact $(\delta t_m^{\mathrm{PE}} - \delta t_m^{\mathrm{Ad}})$(ms)
1	−385.7	−386.3	−0.6
2	−372.7	−373.8	−1.1
3	−354.3	−355.5	−1.2
4	−335.3	−334.6	0.7
5	−316.1	−315.9	0.2
6	−297.8	−297.6	0.2
7	−280.5	−280.1	0.4
8	−264.8	−264.4	0.4
9	−250.3	−251.5	−1.2
10	−237.1	−236.7	0.4

Table 7. Modal travel time perturbation for case A8+(DC=+12.5 m/s) at 50 Hz.

M	Adiabatic δt_m^{Ad}(ms)	MOSPEF δt_m^{PE}(ms)	Coupling impact $(\delta t_m^{\mathrm{PE}} - \delta t_m^{\mathrm{Ad}})$(ms)
1	−717.3	−680.2	37.1
2	−725.9	−561.1	164.8
3	−744.3	−681.3	63.0
4	−811.7	−704.0	107.7
5	−713.8	−699.4	14.4
6	−742.7	−756.8	−14.1
7	−677.2	−682.0	−4.8
8	−647.6	−646.4	1.2
9	−614.0	−615.1	−1.1
10	−582.4	−582.1	0.3

Table 8. Modal travel time perturbation for case B8+
(DC=+12.5 , off-axis Ze=700 m, 50 Hz)

	Modal travel time perturbation (ms)				
m	Linear Adiabatic	Nonlinear Adiabatic	MOSPEF	Nonlinearity Ne (%)	Couplin impact Δt(PE-Ad) (ms)
1	-683.5	-387.6	-387.2	76.4	0.4
2	-670.3	-391.7	-391.0	71.1	0.7
3	-650.6	-399.1	-398.1	63.0	1.0
4	-628.3	-409.2	-407.9	53.6	1.3
5	-605.9	-421.2	-419.5	43.9	1.6
6	-584.5	-434.1	-432.5	34.7	1.6
7	-564.9	-448.4	-446.5	26.0	1.9
8	-546.7	-463.1	-460.7	18.1	2.4
9	-530.1	-477.6	-475.0	11.0	2.6
10	-514.7	-491.1	-488.1	4.8	3.0

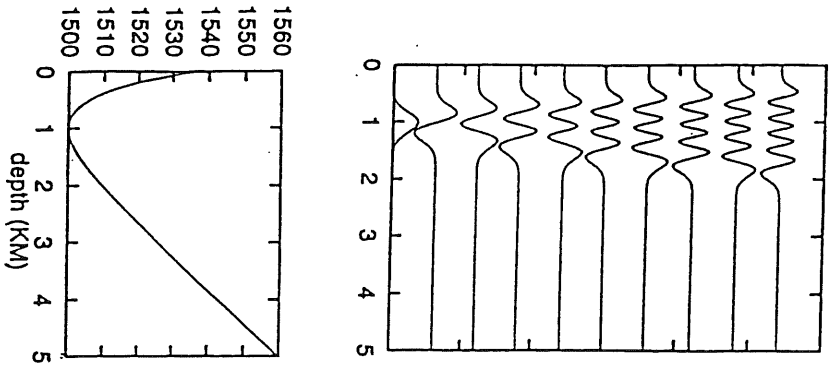

(a) Munk's canonical profile

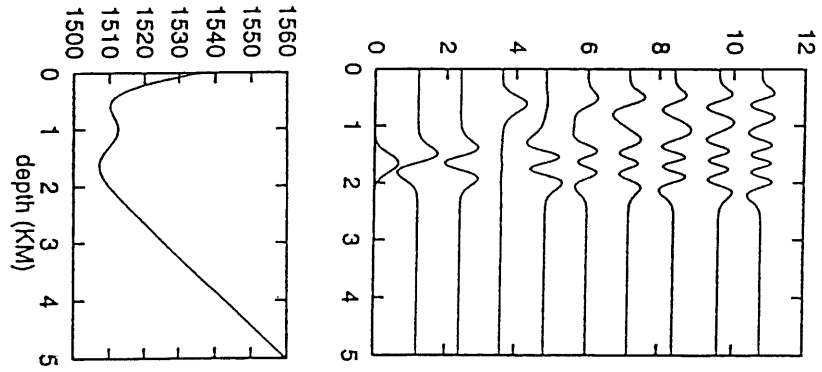

(b). Eddy center of case A8+

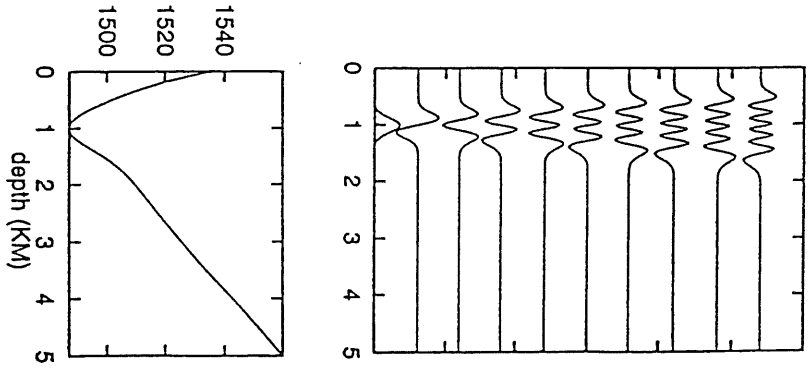

(c). Eddy center of case A8-

Fig.1 Sound speed profile and corresponding local modes (m=1-10) at 50 Hz.

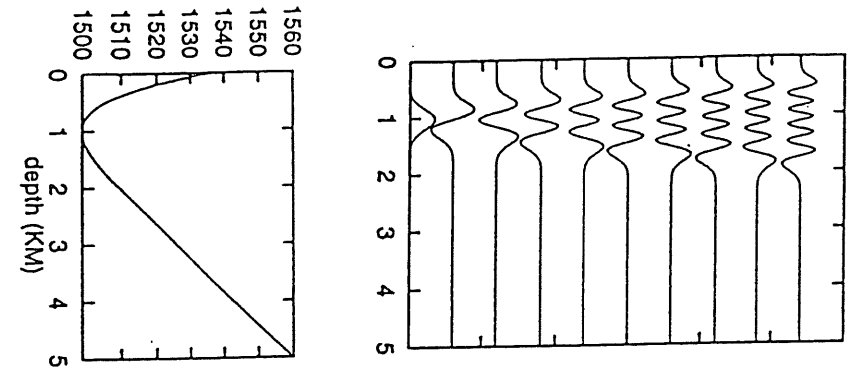

(a). Munk's canonical profile

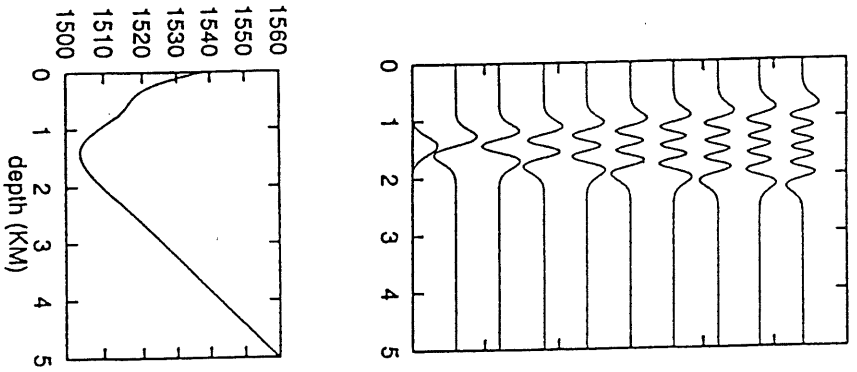

(b). Eddy center of case B8+

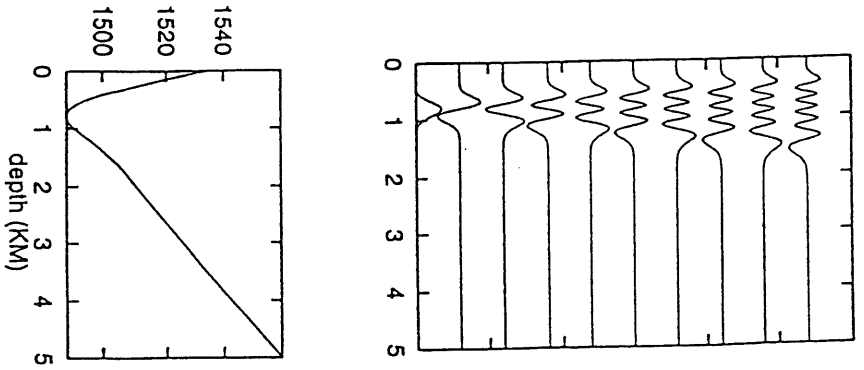

(c). Eddy center of case B8-

Fig.2 Sound speed profile and corresponding local modes (m=1-10) at 50 Hz. (off-axis Ze=700 m)

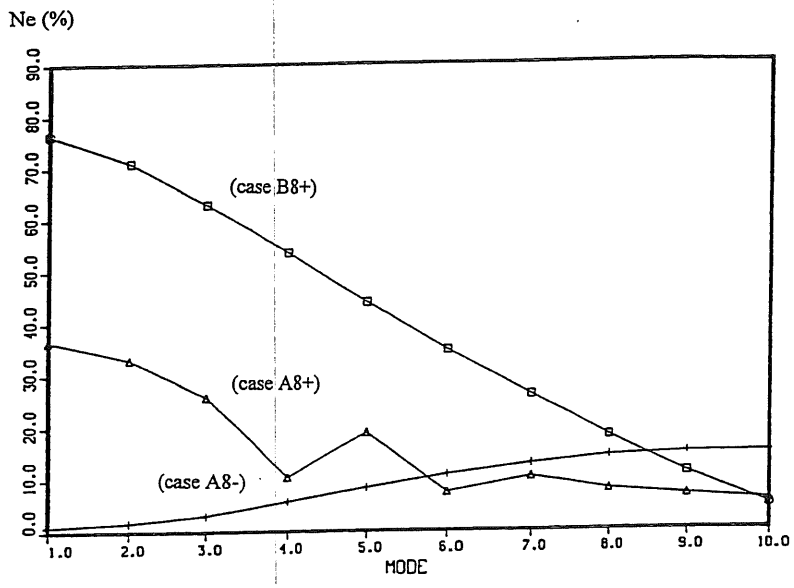

Fig.3 The nonlinearity of modal travel time perturbation versus mode number for strong eddy at frequency f= 50 Hz.
+ (on-axis cold, DC= -12.5 m/s, case A8-)
△ (on-axis warm, DC= +12.5 m/s, case A8+)
□ (off-axis warm, DC= +12.5 m/s, case B8+)

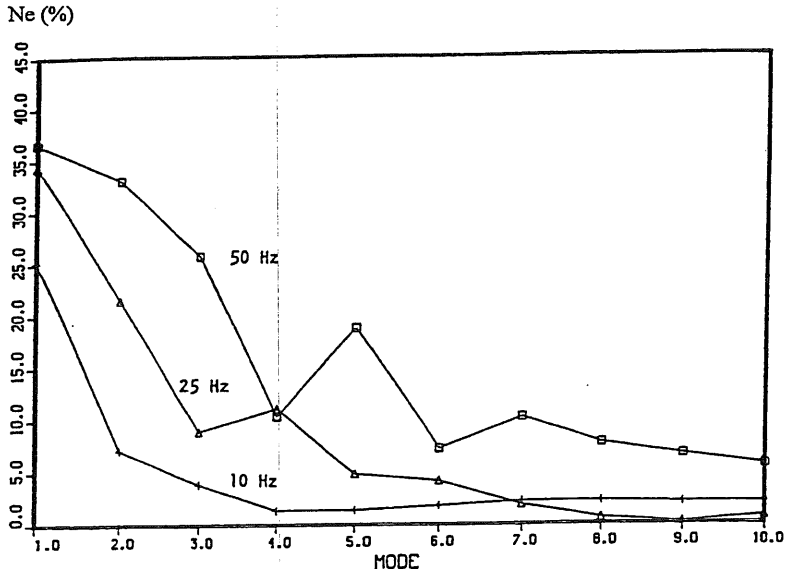

Fig.4 The frequency dependency of nonlinearity of modal travel time perturbation for strong eddy (case A8+) at 50 Hz.

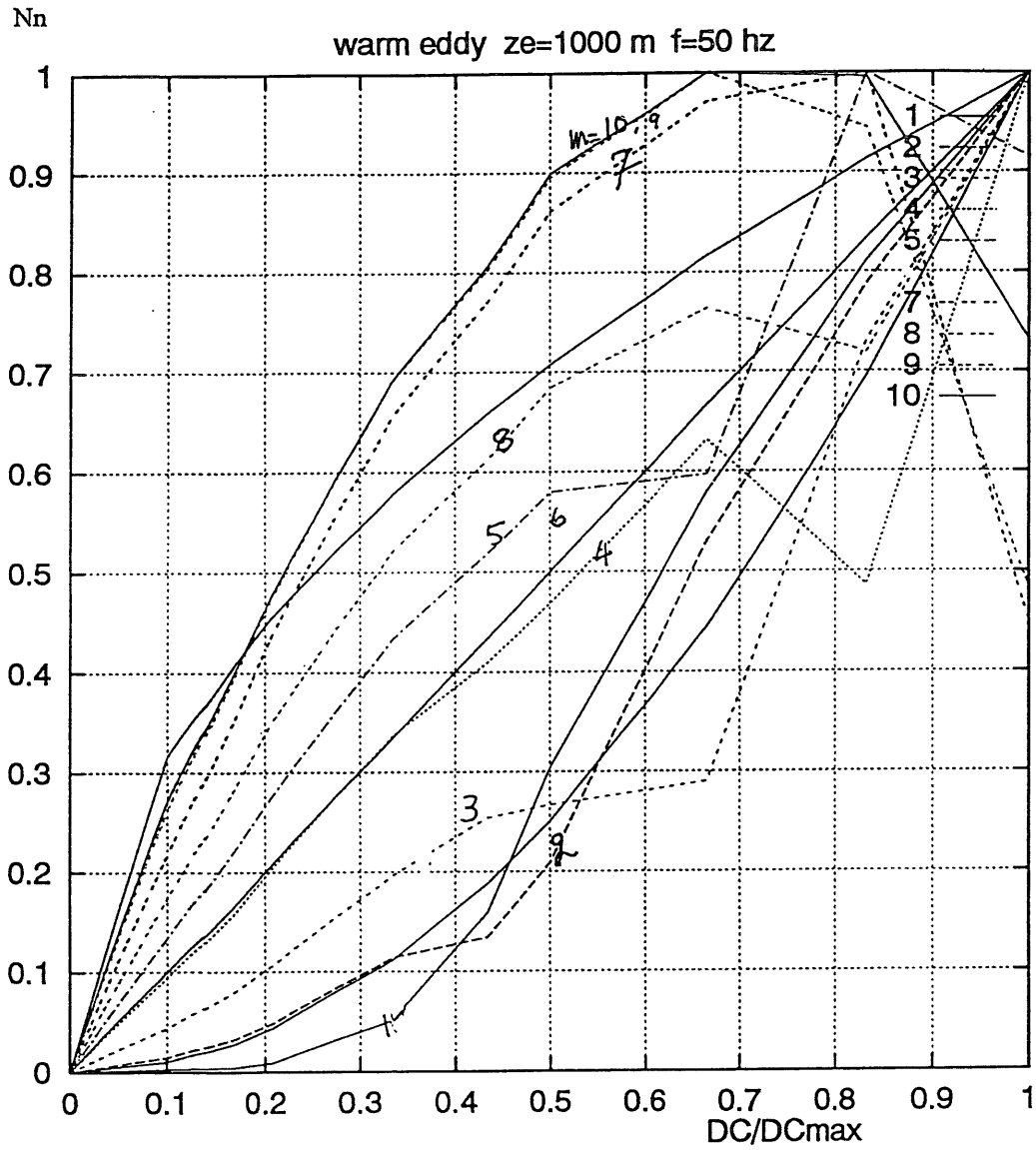

Fig.5 The normalized nonlinearity versus normalized eddy strength for warm on-axis eddy at 50 Hz.

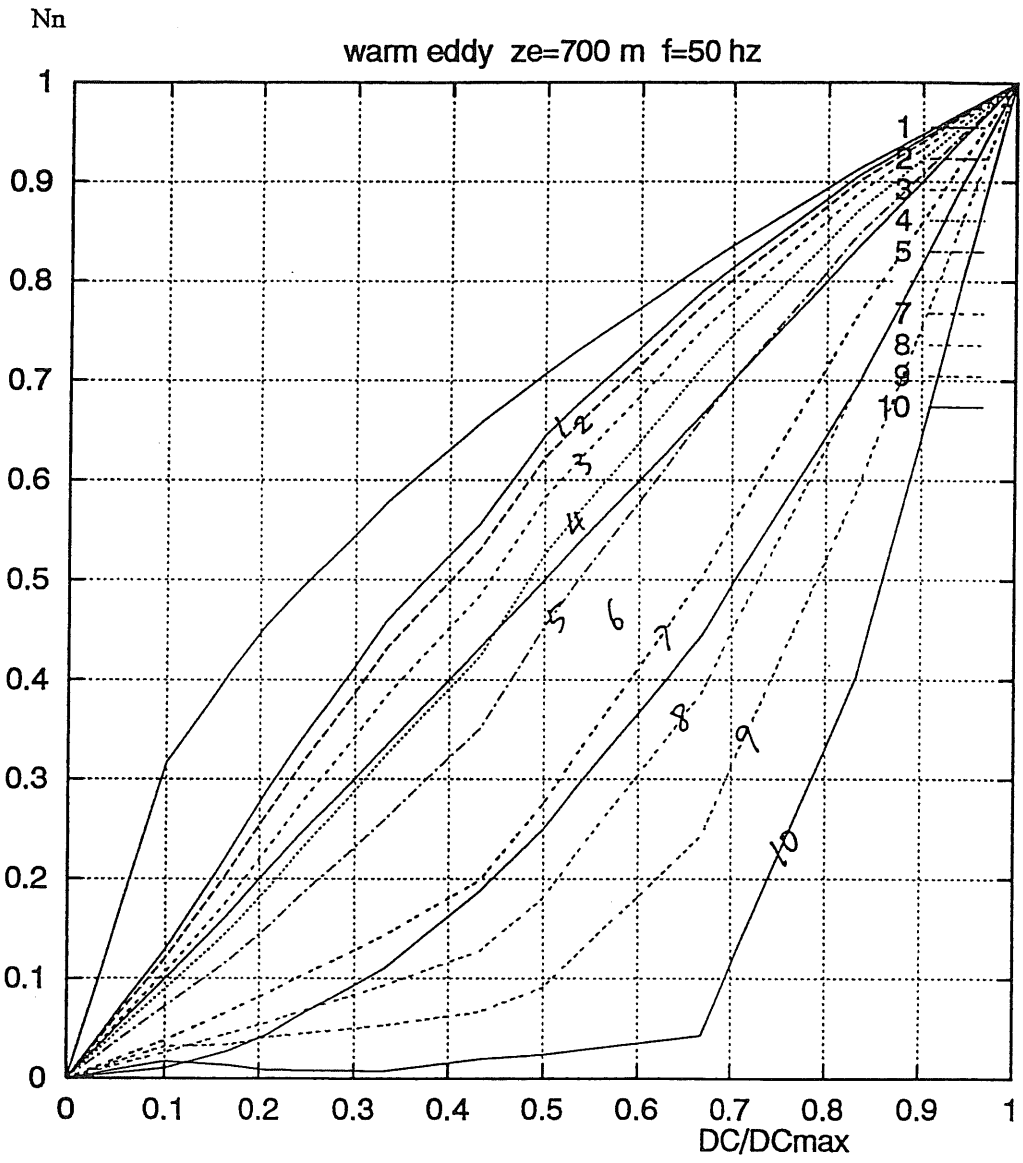

Fig.6 The normalized nonlinearity versus normalized eddy strength for warm off-axis eddy at 50 Hz.

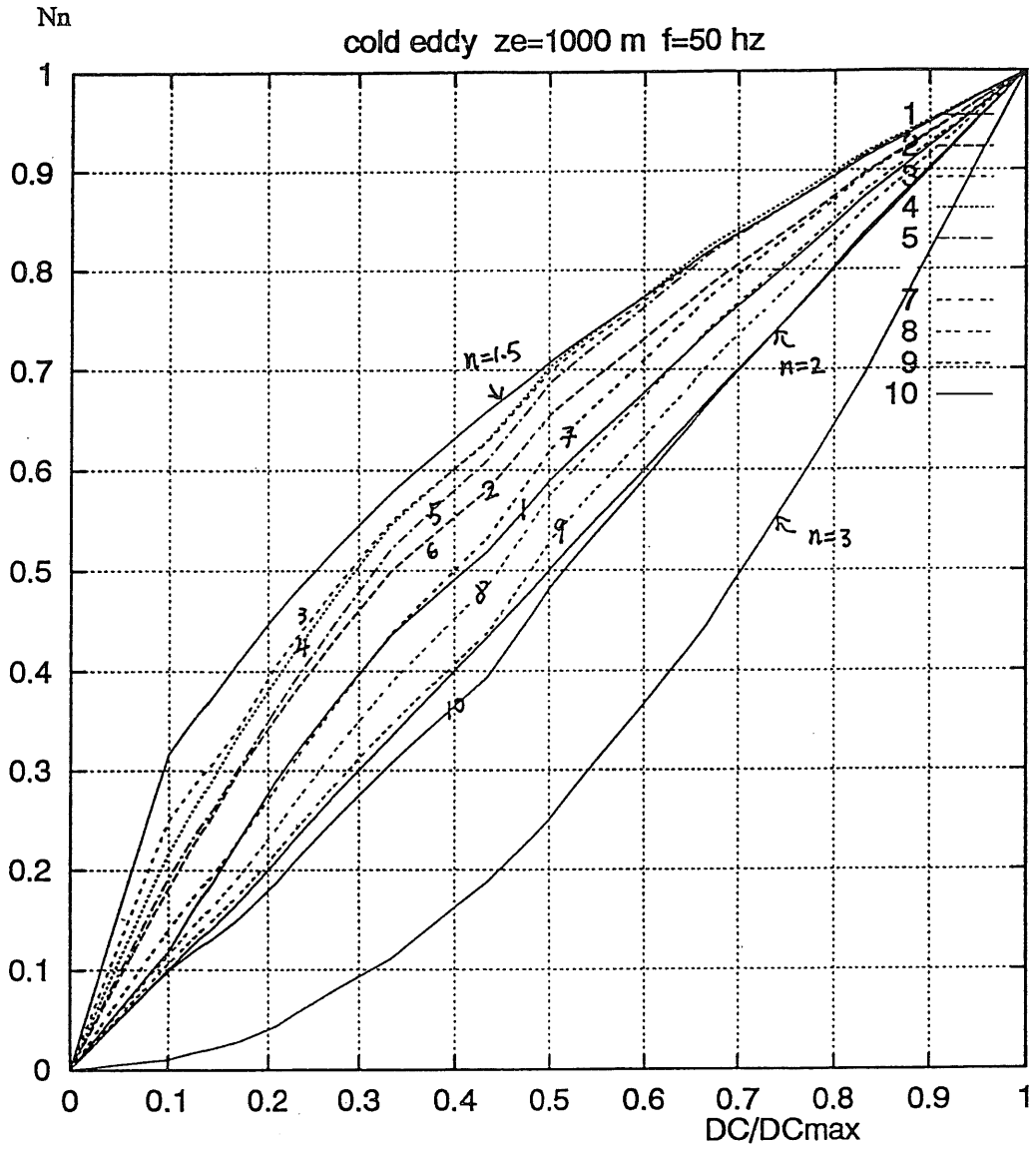

Fig.7 The normalized nonlinearity versus normalized eddy strength for cold on-axis eddy at 50 Hz.

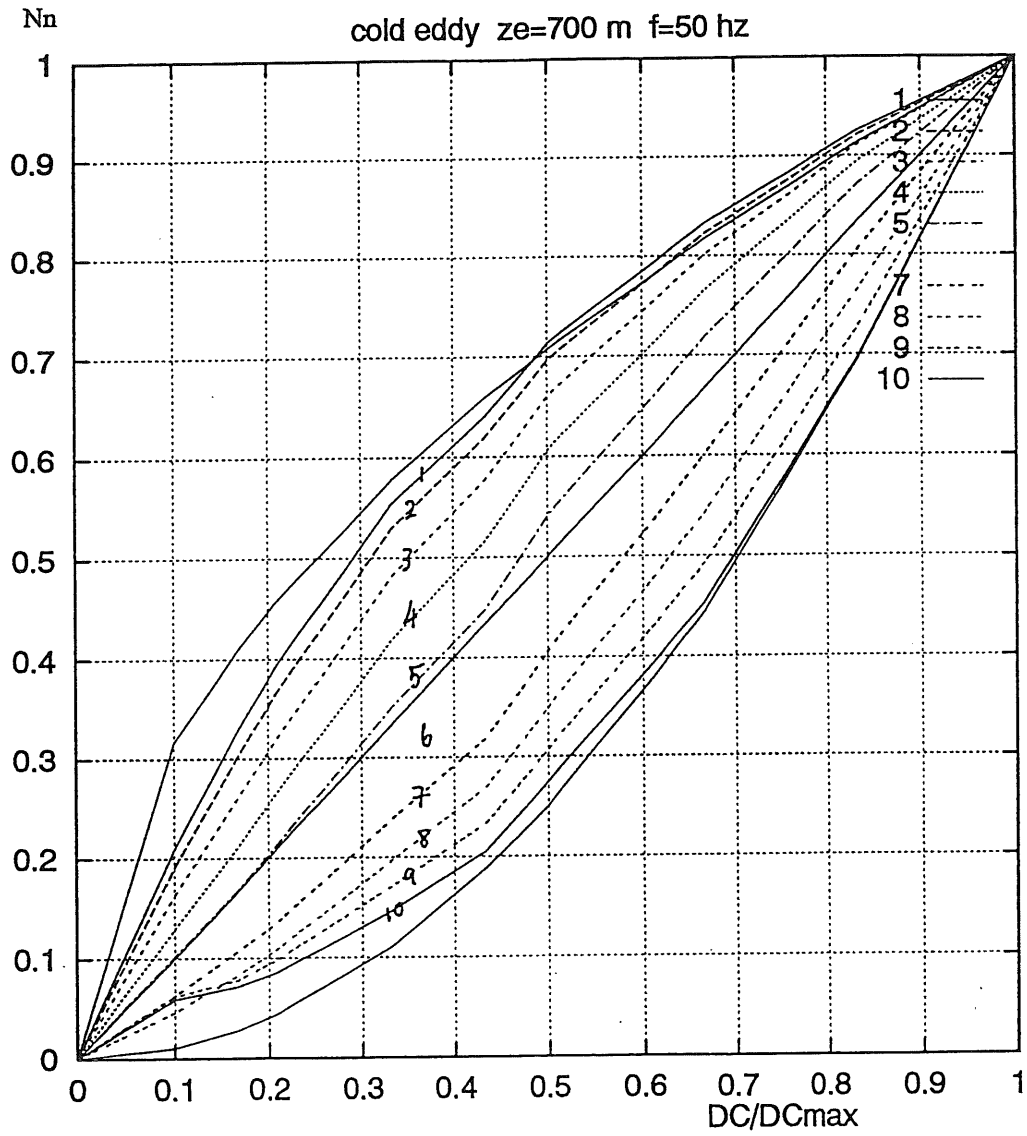

Fig.8 The normalized nonlinearity versus normalized eddy strength for cold off-axis eddy at 50 Hz.

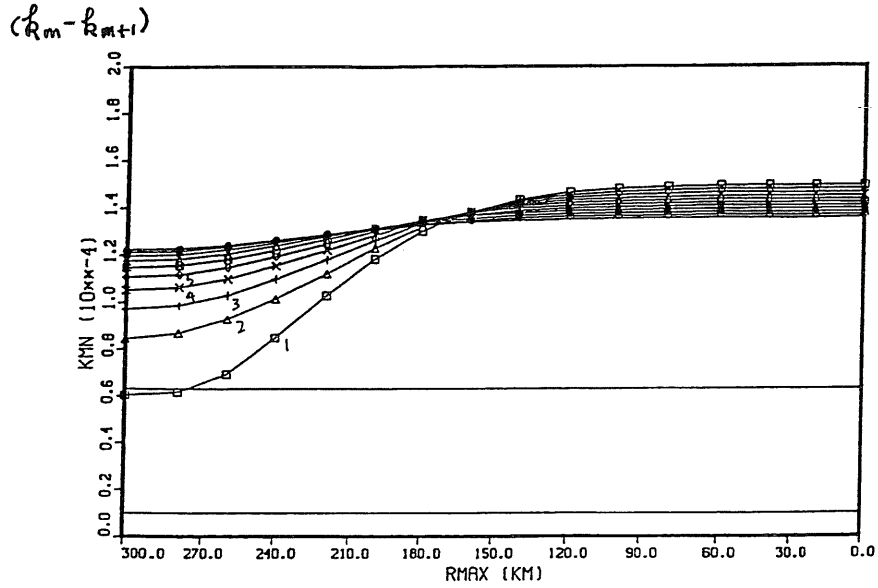

Fig.9 The modal wave number difference (K_m- K_{m+1}) at 50 Hz for case A4+ (DC=5.0 m/s , on-axis), RMAX=300 km is eddy center and RMAX=200 km is the edge of eddy.

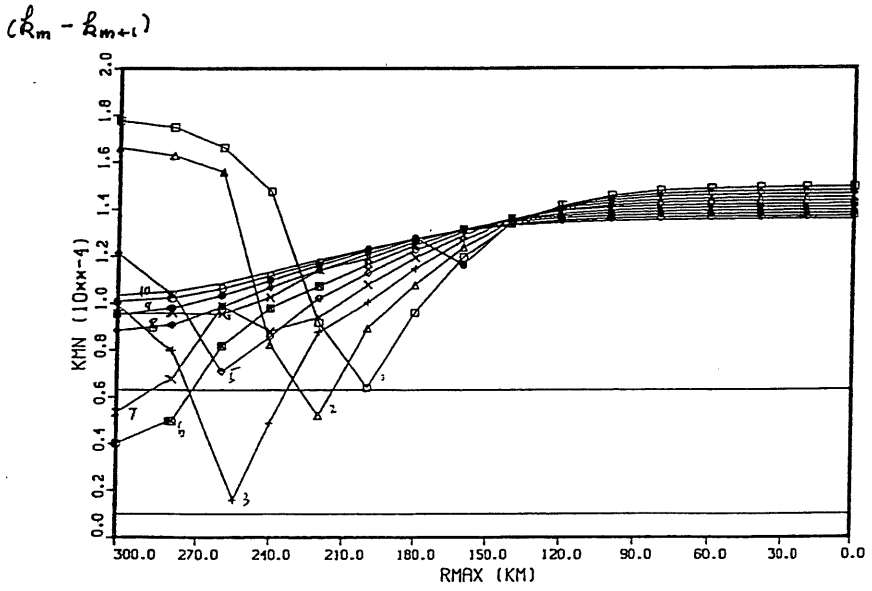

Fig.10 The modal wave number difference (K_m- K_{m+1}) at 50 Hz for case A8+ (DC=12.5 m/s, on-axis), RMAX=300 km is eddy center and RMAX=200 km is the edge of eddy.

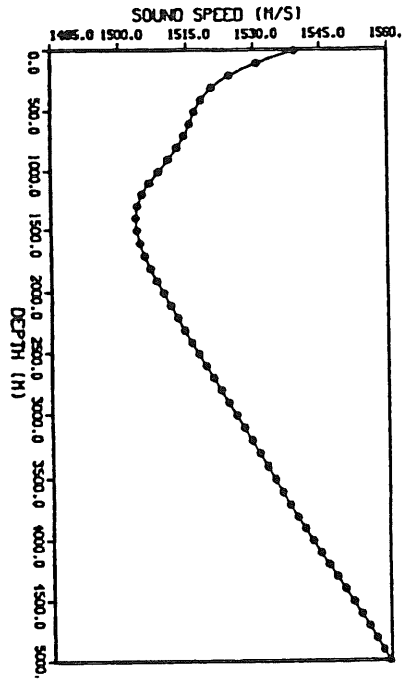

(a)

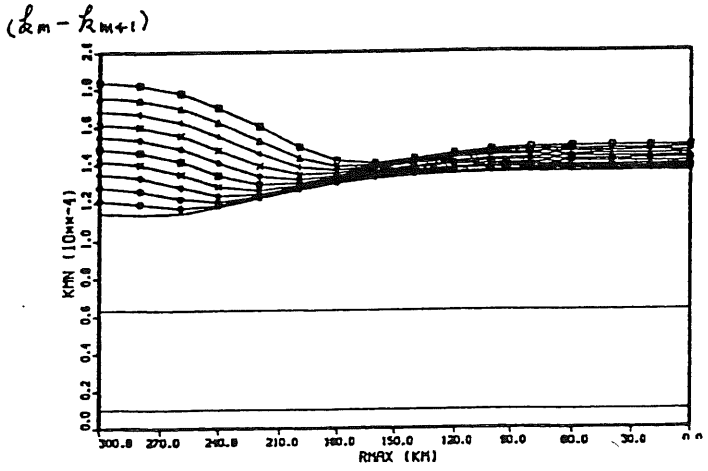

(b)

Fig.11 (a). The SSP for case B8+ (DC= +12.5 m/s, Ze=700 m),
(b). The corresponding modal wave number difference.

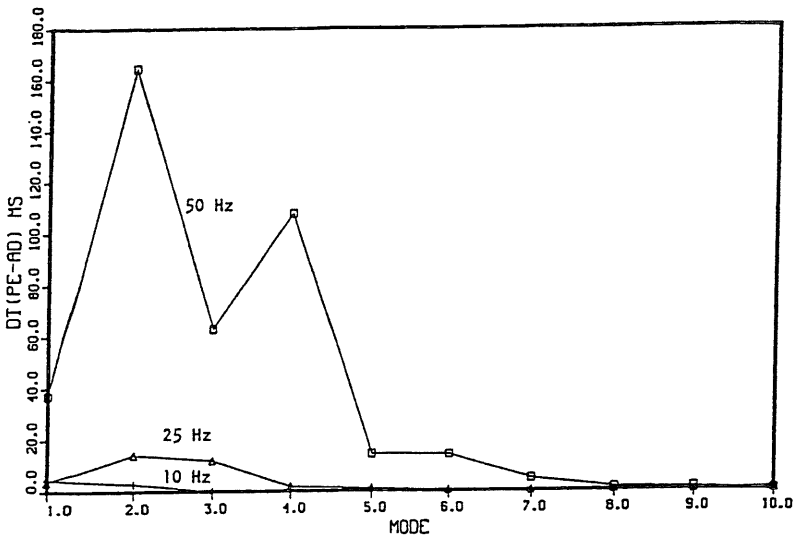

Fig.12 The frequency dependency of mode-coupling impact on modal travel time perturbation for strong eddy (case A8+).